

Enhanced spontaneous Raman scattering in silicon photonic crystal waveguides on insulator

Xavier Checoury, Moustafa El Kurdi, Zheng Han and Philippe Boucaud

Institut d'Électronique Fondamentale, CNRS Univ Paris Sud XI, Bâtiment 220, F-91405 Orsay Cedex, France

xavier.checoury@ief.u-psud.fr

Abstract: We study the spontaneous Raman scattering in a W1 photonic crystal waveguide on silicon-on-insulator where the lower silica cladding remains. Despite the vertical asymmetry that exists in such a waveguide, we numerically and experimentally show that the propagation losses at the pump and the Stokes wavelengths remain low enough to allow a significant exaltation of the spontaneous Raman scattering. In particular, we observe a reshaping of the Raman spectrum and a more than ten-fold enhancement of the Raman scattering efficiency in a W1 photonic crystal waveguide as compared to a single-mode ridge waveguide.

© 2008 Optical Society of America

OCIS codes: (130.5296) Photonic crystal waveguides; (230.5298) photonic crystals

References and links

1. O. Boyraz and B. Jalali, "Demonstration of a silicon Raman laser," *Opt. Express* **12**, 5269–5273 (2004).
2. H. S. Rong, R. Jones, A. S. Liu, O. Cohen, D. Hak, A. Fang, and M. Paniccia, "A continuous-wave Raman silicon laser," *Nature* **433**, 725–728 (2005).
3. H. S. Rong, S. B. Xu, O. Cohen, O. Raday, M. Lee, V. Sih, and M. Paniccia, "A cascaded silicon Raman laser," *Nature Photonics* **2**, 170–174 (2008).
4. J. I. Dadap, R. L. Espinola, R. M. Osgood, S. J. McNab, and Y. A. Vlasov, "Spontaneous Raman scattering in ultrasmall silicon waveguides," *Opt. Letters* **29**, 2755–2757 (2004).
5. R. L. Espinola, J. I. Dadap, R. M. Osgood, S. J. McNab, and Y. A. Vlasov, "Raman amplification in ultrasmall silicon-on-insulator wire waveguides," *Opt. Express* **12**, 3713–3718 (2004).
6. S. Assefa and Y. A. Vlasov, "High-order dispersion in photonic crystal waveguides," *Opt. Express* **15**, 17,562–17,569 (2007).
7. J. E. McMillan, X. D. Yang, N. C. Panoiu, R. M. Osgood, and C. W. Wong, "Enhanced stimulated Raman scattering in slow-light photonic crystal waveguides," *Opt. Letters* **31**, 1235–1237 (2006).
8. K. Inoue, H. Oda, A. Yamanaka, N. Ikeda, H. Kawashima, Y. Sugimoto, and K. Asakawa, "Dramatic density-of-state enhancement of Raman scattering at the band edge in a one-dimensional photonic-crystal waveguide," *Phys. Rev. A* **78**, 011805 (2008).
9. H. Oda and K. Inoue, "Observation of Raman scattering in GaAs photonic-crystal slab waveguides," *Optics Express* **14**, 6659–6667 (2006).
10. H. Oda, K. Inoue, A. Yamanaka, N. Ikeda, Y. Sugimoto, and K. Asakawa, "Light amplification by stimulated Raman scattering in AlGaAs-based photonic-crystal line-defect waveguides," *Appl. Phys. Lett.* **93**, 051114 (2008).
11. J. McMillan, M. Yu, D.-L. Kwong and C. W. Wong "Demonstration of Enhanced Spontaneous Raman Scattering in Slow-Light Silicon Photonic Crystal Waveguides" Conference on Lasers and Electro-Optics/Quantum Electronics and Laser Science Conference and Photonic Applications Systems Technologies, OSA Technical Digest (CD) (2008), paper QMI6.
12. X. Checoury, P. Crozat, J. M. Lourtioz, C. Cuisin, E. Derouin, O. Drisse, F. Poigt, L. Legouezigou, O. Legouezigou, P. Pommereau, G. H. Duan, O. Gauthier-Lafaye, S. Bonnefont, D. Mulin, F. Lozes-Dupuy, and A. Talneau, "Single-mode in-gap emission of medium-width photonic crystal waveguides on InP substrate," *Opt. Express* **13**, 6947–6955 (2005).

13. X. Checoury, P. Boucaud, J. M. Lourtioz, O. Gauthier-Lafaye, S. Bonnefont, D. Mulin, J. Valentin, F. Lozes-Dupuy, F. Pommereau, C. Cuisin, E. Derouin, O. Drisse, L. Legouezigou, F. Lelarge, F. Poingt, G. H. Duan, and A. Talneau, "1.5 μm room-temperature emission of square-lattice photonic-crystal waveguide lasers with a single line defect," *Appl. Phys. Lett.* **86** (2005).
14. Q. Lin, O. J. Painter, and G. P. Agrawal, "Nonlinear optical phenomena in silicon waveguides: Modeling and applications," *Opt. Express* **15**, 16,604–16,644 (2007).
15. M. El Kurdi, X. Checoury, S. David, T. P. Ngo, N. Zerounian, P. Boucaud, O. Kermarrec, Y. Campidelli, and D. Bensahel, "Quality factor of Si-based photonic crystal L3 nanocavities probed with an internal source," *Opt. Express* **16**, 8780–8791 (2008).
16. X. Li, P. Boucaud, X. Checoury, O. Kermarrec, Y. Campidelli, and D. Bensahel, "Probing photonic crystals on silicon-on-insulator with Ge/Si self-assembled islands as an internal source," *J. Appl. Phys.* **99**, 023103 (2006).
17. S. David, M. El kurdi, P. Boucaud, A. Chelnokov, V. Le Thanh, D. Bouchier, and J. M. Lourtioz, "Two-dimensional photonic crystals with Ge/Si self-assembled islands," *Appl. Phys. Lett.* **83**, 2509–2511 (2003).
18. S. J. McNab, N. Moll, and Y. A. Vlasov, "Ultra-low loss photonic integrated circuit with membrane-type photonic crystal waveguides," *Opt. Express* **11**, 2927–2939 (2003).
19. M. Settle, M. Salib, A. Michaeli, T. F. Krauss, "Low loss silicon on insulator photonic crystal waveguides made by 193nm optical lithography," *Opt. Express* **14**, 2440–2445 (2006).

1. Introduction

Silicon photonics offers the promise of low-cost and high frequency devices due to its potentially high degree of integration as well as to its large optical bandwidth. Despite the recent advances in the field of silicon photonics, the fabrication of active optical functions and, in particular, the fabrication of lasers remains one of the most difficult task. Until now, except for the approaches that use III-V materials, only the use of a nonlinear effect, the stimulated Raman scattering, has allowed to obtain a laser effect in a rib waveguide etched on a silicon-on-insulator (SOI) substrate [1, 2]. One of the limitations of these reported Raman scattering studies is that it requires long cavities (> 1 cm) or high Q factor ring cavities with large area (≈ 1 cm²) to achieve the gain required by the laser effect [2, 3]. To overcome this limitation, that is incompatible with the on-chip integration of these components, photonic crystals (PhCs) appear as compact alternatives. Photonic crystal waveguides in SOI can strongly confine light due to their reduced width and height in a manner similar to photonic wires in which spontaneous and stimulated Raman scattering has already been observed in SOI [4, 5]. Moreover, the existence of slow modes in PhCs, the group velocity of which can be 100 times smaller than the light in vacuum [6], can theoretically enhance further the spontaneous scattering [7, 8]. Recently, some results have been reported in 1-mm long PhCs made in suspended AlGaAs membranes [8, 9, 10] and in Si membranes [11]. In this work, we demonstrate the enhancement of the spontaneous Raman scattering in PhC waveguides on SOI compared to photonic wires of similar dimension. Contrary to refs. [8, 9, 10, 11], the present waveguides are short (50 μm long) and made in SOI where the oxide below the PhC has not been removed. Doing so, we do not rely on the fragile membrane structures that are incompatible with a good thermal dissipation and with the on-chip integration. We show a more than ten-fold enhancement of the Raman scattering efficiency in a W1 photonic crystal waveguide as compared to a single mode ridge waveguide.

2. Simulation

Figure 1 shows the calculated band diagram of a W1 waveguide made by omitting one row of holes in the ΓK direction. The hole radius r and the Si layer thickness d are $0.25a$ and $0.45a$ respectively where a is the lattice constant. The buried oxide (BOx) layer has a thickness of $4.5a$ (i.e. 2 μm for a lattice constant of 440 nm). 3D-FDTD with Bloch boundary conditions in the direction of the waveguide and with perfectly matched layers (PML) on the other directions has been used for the computation [12, 13]. The normalized frequencies that are used in the

experimental setup for the pump and the signal (i.e. Stokes) frequencies are 0.28 and 0.258 respectively. Their difference is 15.6 THz, i.e. the energy of the zone center optical phonon in silicon. We use the slow group velocity mode of the W1, near the cut-off frequency of 0.26 to enhance the spontaneous Raman scattering since the scattering efficiency is inversely proportional to the group velocity of the Stokes mode [7, 8].

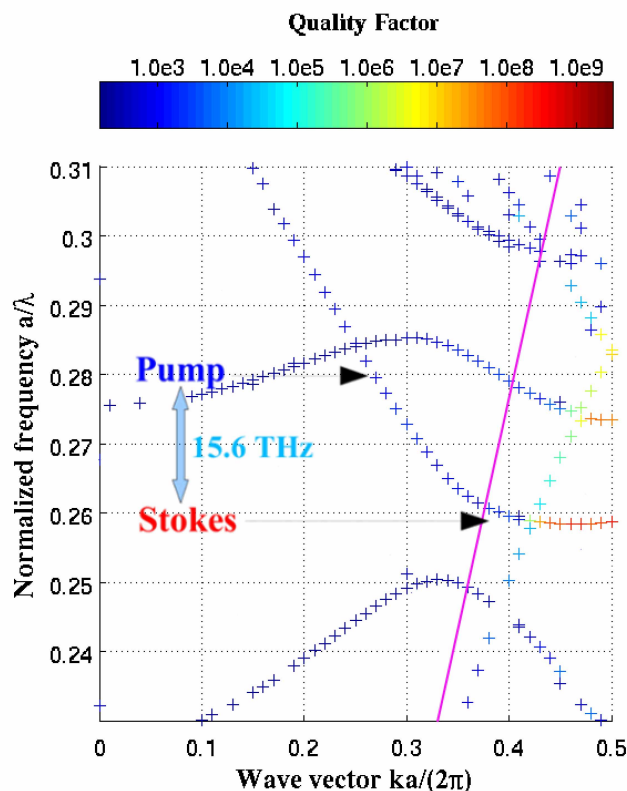


Fig. 1. Band diagram of the W1 PhC silicon-on-insulator waveguide calculated by 3D-FDTD. The pump and Stokes normalized frequencies are indicated as well as the quality factor of the mode $Q = \omega\tau$ where ω is the pulsation and τ is the life-time of the mode. The silica light line is represented in violet.

Because the Raman linewidth in silicon is only 105 GHz at room temperature [14], we do not try to slow down the pump mode despite the fact that a slow group velocity of the pump mode also enhances the scattering efficiency. In doing so, we avoid the difficult fabrication of a PhC waveguide where the frequency separation of the pump and Stokes modes would be controlled with an accuracy better than one percent which is the ratio of the Raman linewidth to the separation of the pump and Stokes frequencies. Instead, we used the ordinary fundamental mode of a W1 waveguide to easily tune the pump and as a consequence the Stokes wavelength. As seen, the chosen pump frequency resides above the silica light cone while the Stokes mode is below. Despite the fact that the pump mode is not a truly guided mode, the losses remain moderate if we use short PhC waveguide. Indeed, using the calculated quality factor $Q = \omega\tau$ of these modes, where ω is the pulsation and τ is the power decay time of the mode computed by 3D-FDTD, losses of the pump mode can be estimated to be $l = 1/(v_{gn}c\tau)$ that is

$l = (2\pi\omega_n)/(Qav_{ng}) \text{ cm}^{-1}$ where $v_{ng} = \frac{d\omega}{cdk}$ is the normalized group velocity of the mode, ω_n its normalized frequency, c is the speed of light and a is the lattice constant expressed in cm. According to the 3D-FDTD, the propagation loss for the pump mode can be estimated to be around 150 cm^{-1} that represents a 3.5 dB loss for a $50 \mu\text{m}$ long waveguide. The calculation of the losses below the silica light line does not make sense since losses are mainly induced by the disorder in the fabricated structure and they are not taken into account in the simulation of a perfectly periodic waveguide.

3. Experiment

The investigated structures were fabricated from a silicon-on-insulator substrate with a buried oxide thickness of 2 μm . The PhC waveguide were fabricated in the 110 direction of a SOI wafer. The thickness of the Si layer above the buried oxide is 200 nm. The sample was coated with a resist mask and photonic crystal patterns were designed by e-beam lithography using a 30 kV Raith Elphy writer [15, 16, 17]. The designed photonic crystal waveguide has a length of $50 \mu\text{m}$, a lattice period of 452 nm and an air hole radius equal to $0.25a$. W1 waveguides were classically fabricated in triangular lattice patterns by omitting to drill one row of holes along the ΓK direction. In order to measure this short PhC waveguide, two access ridge waveguides are butt coupled. They are $220 \mu\text{m}$ long and comprise two sections. The first one, the length of which is $160 \mu\text{m}$, is a straight section of a 450-nm wide single mode waveguide. The second one is a $60 \mu\text{m}$ long tapered waveguide with a width varying from 450 nm to 780 nm to match the 780-nm width of the W1 waveguide in a manner similar to the reference [18] (see inset Fig. 2). The holes as well as the ridge waveguides were etched through the silicon matrix by inductively coupled reactive ion etching. The buried oxide was not removed to allow a good thermal dissipation under high power excitation as well as mechanical stability. Polarization maintaining lensed optical fibers with spot diameter of $\approx 2.5 \mu\text{m}$ are used to collect and inject light. To observe the Raman scattering, a tunable laser source and an erbium doped fiber amplifier are used. Band-pass filters allow to remove the spontaneous emission from the pump as well as to remove the pump wavelength from the output signal.

Figure 2 represents the transmission spectra of the W1 waveguide measured with a spontaneous emission source and an optical spectrum analyzer (OSA). The light and dark gray areas indicate the frequency range swept for the pump and the Stokes signal respectively. The insertion loss for the pump signal is around 7.5 dB. The propagation losses have been measured to be 4 dB using similar W1 waveguides of different lengths. This value, in good agreement with the simulations, allows to deduce the coupling losses that are equal to 1.5 dB at each end of the W1 waveguide. The dip around 1610 nm is due to the coupling of the fundamental mode of the W1 with a higher-order slow mode at the computed normalized frequency of 0.274. The crossings of the W1 slow-mode with the silica light line and with the first-guided TM-like mode occur at 1647 nm and at 1656 nm respectively. They are responsible for the two dips observed in the transmission spectra at these wavelengths.

As expected, a small window between 1656 nm and 1666 nm exists where the propagation losses as well as the group velocity are low. The insertion losses in this range are above 13 dB. In this frequency range, we were not able to measure significant propagation losses even with $100 \mu\text{m}$ long W1 waveguide, the maximum length allowed by our e-beam lithography without introducing stitching errors. However, this result is in agreement with reported measurements on W1 waveguides in SOI for which propagation losses are around 100 dB/cm [19]. Because the waveguide considered here is only $50\text{-}\mu\text{m}$ long, the propagation losses can be estimated to be below 0.5 dB and the insertion losses are due to the weak coupling between the ridge and W1 waveguides at moderate ($\approx c/30$) low-group velocities in the PhC.

A closed view of this area is represented in Fig. 3 (black curve) on a linear scale. From the

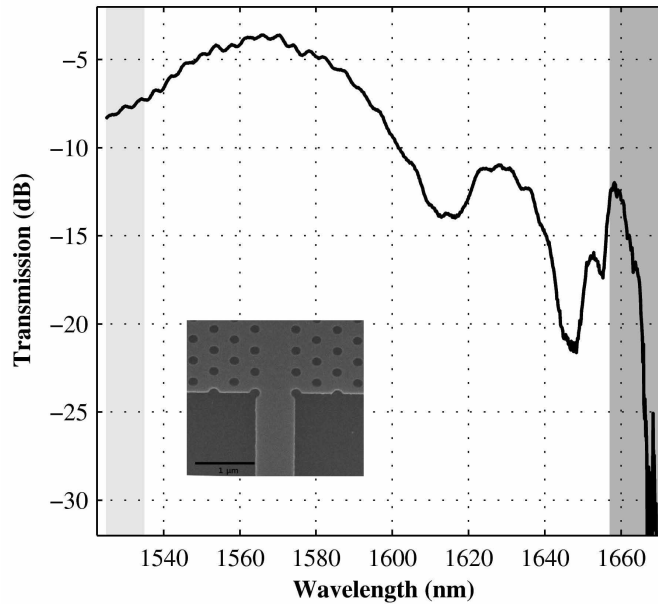


Fig. 2. Transmission spectrum of the W1 waveguide measured with a spontaneous emission source and an optical spectrum analyzer (OSA) with a resolution of 0.5 nm. The light and dark gray areas represent the frequency range swept for the pump and the Stokes signal respectively. Inset: scanning electron microscope view of the termination of a PhC waveguide

Fabry-Pérot interference fringes, the group velocity can be deduced to be between $c/25$, near 1658 nm, and $c/40$, near 1666 nm. The gray curve represents the measured spectra when the PhC waveguide is pumped with a tunable laser at $\lambda = 1530.7$ nm and an erbium amplifier without any band-pass filter to remove the source spontaneous emission. The coupled pump power in the PhC waveguide is estimated to be 24 mW. As seen, a Raman signal clearly emerges above the spontaneous emission of the source at $\lambda = 1663$, i.e. at 15.6 THz below the pump frequency. Despite the 100 times higher power coupled into the waveguide, the Fabry-Pérot fringes are shifted by only 0.2 nm towards long wavelengths. Note also that the measured power at the pump wavelength at the output of the waveguides varies linearly with the incident power. These two facts indicate that thermal effects as well as the losses induced by photo-generated free-carriers remain negligible.

Since the spontaneous emission from the source can easily be filtered, we need to distinguish between the Raman signal generated in the ridge access waveguides and the one generated in the PhC alone. Figure 4 shows the spectra measured for various pump wavelengths when a band-pass filter removes the spontaneous emission from the pump source. With the filter, the coupled power into the PhC waveguide is 12.5 mW. For a pump wavelength of 1535.8 nm, the Stokes wavelength is inside the W1 band gap at 1669.2 nm. The spectra of the spontaneous Raman generated inside the waveguide is represented in black in Fig. 4. The Raman scattering generated in the input ridge waveguide is blocked by the W1 and no scattering occurs in the PhC waveguide since no guided mode is allowed. As a consequence, only the Raman scattering generated in the output ridge waveguide is collected. The full width at half maximum (FWHM) of this Raman spectrum is roughly equal to 1 nm, the expected Raman linewidth in silicon. For wavelengths between 1655 nm and 1666 nm, because the W1 insertion losses are higher than 13 dB (fig. 2), the collected spontaneous Raman scattering power is the sum of the one generated

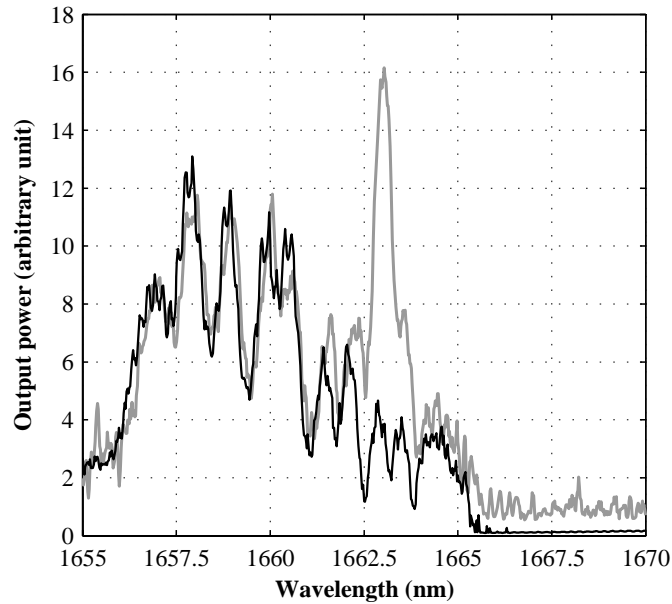


Fig. 3. Output power on a linear scale measured with an optical spectrum analyzer (resolution of 0.5 nm). The source is a wide band low power noise source for the black curve. In the case of the gray curve, a power of 24 mW at 1530.6 nm is coupled in the W1 waveguide from an amplified laser source to generate spontaneous Raman scattering at 1663.1 nm.

in the photonic crystal and in the output ridge waveguide only. Note also that because the 13 dB insertion losses of the W1 waveguide are coupling losses, as mentioned above, the Raman scattering power generated inside the PhC waveguide is 6 dB higher than the actually measured power. The spectra of fig. 4 show how the PhCs strongly modify the scattering emission. In particular, for pump wavelengths of 1530.6 nm and 1531.7 nm, the FWHM are smaller than 0.5 nm, the OSA resolution. Note also that the pump wavelengths are chosen to maximize the Raman scattering at a given frequency, in other words they are chosen so that the Stokes wavelength coincides with a Fabry-Pérot maximum of the W1 waveguide.

Subtracting the spontaneous Raman scattering generated inside the output ridge waveguide from the spectra at 1658 nm and at 1664.4 nm, we respectively get a collected Stokes power of 1.45 pW and of 4 pW. From 1658 nm to 1665 nm, the group velocity varies from $c/25$ to $c/40$ while the Raman scattering efficiency is roughly multiplied by 2.7. This results seems to indicate a dependence of the Raman power with v_g^{-2} rather than with v_g^{-1} . The reason is that the collected power depends on two effects related to v_g^{-1} : the enhancement of the Raman scattering inside the photonic crystal due to the slow-wave effect and the enhancement of the reflectivity due to the mismatch of the group velocities at the interface between the PhC waveguide and the ridge waveguide. Note also that the propagation losses in the photonic crystal increase when v_g decreases and can attenuate the enhancement of the Raman spontaneous emission.

To compare the spontaneous Raman scattering generated in the W1 waveguide and the one generated in the output ridge waveguide, we consider the differential equation obeyed by the spontaneous Raman power P_s (ref. [4]):

$$\frac{dP_s}{dz} = -\alpha_s P_s + \kappa P_p \exp(-\alpha_p z)$$

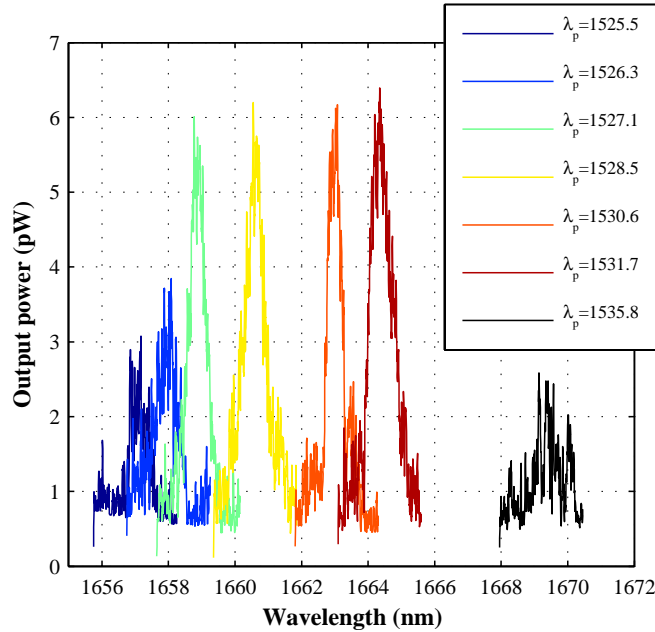


Fig. 4. Spontaneous Raman scattering spectra for various wavelengths of the pump with a coupled power of 12.5 mW in the PhC waveguide. The OSA resolution is 0.5 nm.

where $\alpha_{s(p)}$, is the loss coefficient of the Stokes (pump) signal, κ is the spontaneous Raman coefficient and P_p is the pump power at the input of the waveguide. Neglecting the loss of the Stokes signal in the photonic crystal, the spontaneous Raman coefficient is given by $\kappa = P_s / (P_p L_{\text{eff}})$ with $L_{\text{eff}} = (1 - \exp(-\alpha_p L)) / \alpha_p$, where L is the waveguide length. From the measurement at $\lambda_p = 1531.7$ nm, we get $P_p = 12.5$ mW and $L_{\text{eff}} = 32$ μm . Taking into account that the coupling loss to the PhC waveguide is 6 dB at $\lambda_s = 1664.4$ nm, we get $P_s = 16$ pW for the spontaneous Raman power inside the PhC waveguide from the measurement and a value of κ equal to 4×10^{-7} cm^{-1} . For the ridge waveguide, we get $P_p = 2.7$ mW, $P_s = 1.7$ pW, $L_{\text{eff}} = 220$ μm and κ equal to 2.9×10^{-8} cm^{-1} for the ridge waveguide. This value of κ in the ridge waveguide is smaller than the one reported in the reference [4] because of the enlargement of our ridge waveguide before the photonic crystal that decreases the field intensity of the pump in the guide. Despite the larger modal area of the PhC waveguide than the one of a ridge waveguide, the scattering efficiency in the photonic crystal is thirteen times higher than in the ridge waveguide due to small group velocity effects.

4. Conclusion

We have presented an experimental study of the spontaneous Raman scattering in a silicon photonic crystal W1 waveguide on insulator. We have shown that the Raman scattering spectrum is strongly modified by a 50 μm -long photonic crystal waveguide. For some particular wavelengths of the pump, the FWHM of the Stokes signal can be less than 0.5 nm instead of the 1 nm achieved in a standard ridge waveguide. More importantly, the efficiency of the Raman scattering is increased by more than one order of magnitude due to the small group velocity that increases the light-matter interaction. These results are encouraging for the realization of a silicon photonic crystal laser on insulator where the stimulated Raman scattering may be achieved in a longer W1 waveguide with decreased losses of coupling and propagation.

Acknowledgments

We thank the Région and C'nano Ile de France for financial support of Zheng Han. We thank B. Ghyselen from Soitec for providing SOI wafers.